# Aluminum extracts in Antarctic paleosols: Proxy data for organic compounds and bacteria and implications for Martian paleosols

William C. Mahaney [a,*], Kris M. Hart [b], James M. Dohm [c], Ronald G.V. Hancock [d], Pedro Costa [e], Shane S. O'Reilly [b], Brian P. Kelleher [b], Stephane Schwartz [f], Bruno Lanson [f]

[a] Quaternary Surveys, 26 Thornhill Ave., Thornhill, Ontario, Canada, L4J 1J4
[b] School of Chemical Sciences, Dublin City University, Glasnevin, Dublin 9, Ireland
[c] Department of Hydrology and Water Resources, University of Arizona, Tucson, AZ, 85721, USA
[d] Medical Physics and Applied Radiation Sciences, and Department of Anthropology, McMaster University Hamilton, Ontario, Canada L8S 4K1
[e] Departmento de Geologia, University of Lisbon, Lisbon, Portugal
[f] IS Terre, CNRS, Université of Grenoble I, Grenoble, France

## ABSTRACT

Pyrophosphate-extractable Al has been used to establish the presence of organically-complexed compounds in middle latitude and tropical soils and paleosols on Earth. As proxy data used to establish the presence of organic molecules and trace movement within profiles, it has proved an accurate indicator of downward translocation in Spodosols (podzols). Antarctic paleosols, dating from Middle to Early Miocene age (15–20 Ma), are mineralic weathering profiles lacking A and B horizons. These profiles exhibit pavement/Cox/Cz/Cu horizons, largely with sandy silt textures, little clay, and exceedingly low concentrations of organic matter. Recent chemical investigations of 33 soil samples from the New Mountain and Aztec Mountain areas near the Inland Ice, adjacent to the Taylor Glacier, show that pyrophosphate-extractable Al concentrations vary in phase with organic carbon as determined by loss-on-ignition. While Al-extract concentrations in selected samples are low (<0.15%), increasing values above nil approximately correlate positively with increases in bacterial populations of several common phylum, the extreme high numbers with more advanced biota including fossil Coleoptera. Available data suggest $Al_p$ extracts may target samples which may have undergone minor chelation, and which over long periods of time might have a cumulative weathering effect resulting in the accumulation of small concentrations of organic matter.

As such, $Al_p$ extracts may prove useful in targeting the presence of life once *in situ* investigations of paleosols begin on Mars.

© 2011 Elsevier B.V. All rights reserved.

## 1. Introduction

Major requirements for terrestrial and presumably extraterrestrial microbial life are liquid water, carbon, nitrogen, and iron, the latter as $Fe^{+2}$ or $Fe^{+3}$ (Falkowski et al., 2008). While these requirements complement each other with regard to physiological processes, perhaps more importantly, water increases the mobility of C, N, and to some degree Fe, the latter accelerating the oxidation potential of mineral grains by importing O to sites where $Fe^{+2}$ is converted to $Fe^{+3}$. Both forms of Fe are important in microbial respiration, although $Fe^{+3}$ is more easily taken up by microorganisms such as bacteria and fungi (Pitt, 1979). Fluctuations of organic C and N as organically-complexed material are seen to move in concert with pyrophosphate-extractable Al ($Al_p$) (Mahaney et al., 1999, 2009, 2010a), such that $Al_p$ might be used to signal the presence of microbes when C and N are at detection limits.

Previous work with Cryosols (cold-desert paleosols) in the Antarctic (Fig. 1 for location; Fig. 2A for stratigraphy) showed the presence of microbes in horizons with a Fe/salt mixed composition or in salt-rich zones [(Claridge and Campbell, 1968; Claridge, 1977) (Fig. 2A, arrows indicate the presence of microbial life) rather than other horizons, including ones that are Fe-enriched (Mahaney et al., 2000, 2001)]. Cryosols exist either as discrete profiles or as pedostratigraphic columns, the latter consisting of two or more profiles in succession with the older profile at base descending in age closer to the land surface. The structure of each profile proliferates in space and time as Fe horizon(s) over salt rich horizon(s), the most recent profile in place since at least the mid-Miocene and topped with a pebble pavement depleted of fines by near constant action of wind. Colonies

---

* Corresponding author.
*E-mail addresses:* arkose@rogers.com (W.C. Mahaney), hart.kris2@mail.dcu.ie (K.M. Hart), jmd@hwr.arizona.edu (J.M. Dohm), ronhancock@ca.inter.net (R.G.V. Hancock), ppcosta@fc.ul.pt (P. Costa), shane.oreilly8@mail.dcu.ie (S.S. O'Reilly), brian.kelleher@dcu.ie (B.P. Kelleher), schwartz@ujf-grenoble.fr (S. Schwartz), bruno.lanson@ujf-grenoble.fr (B. Lanson).
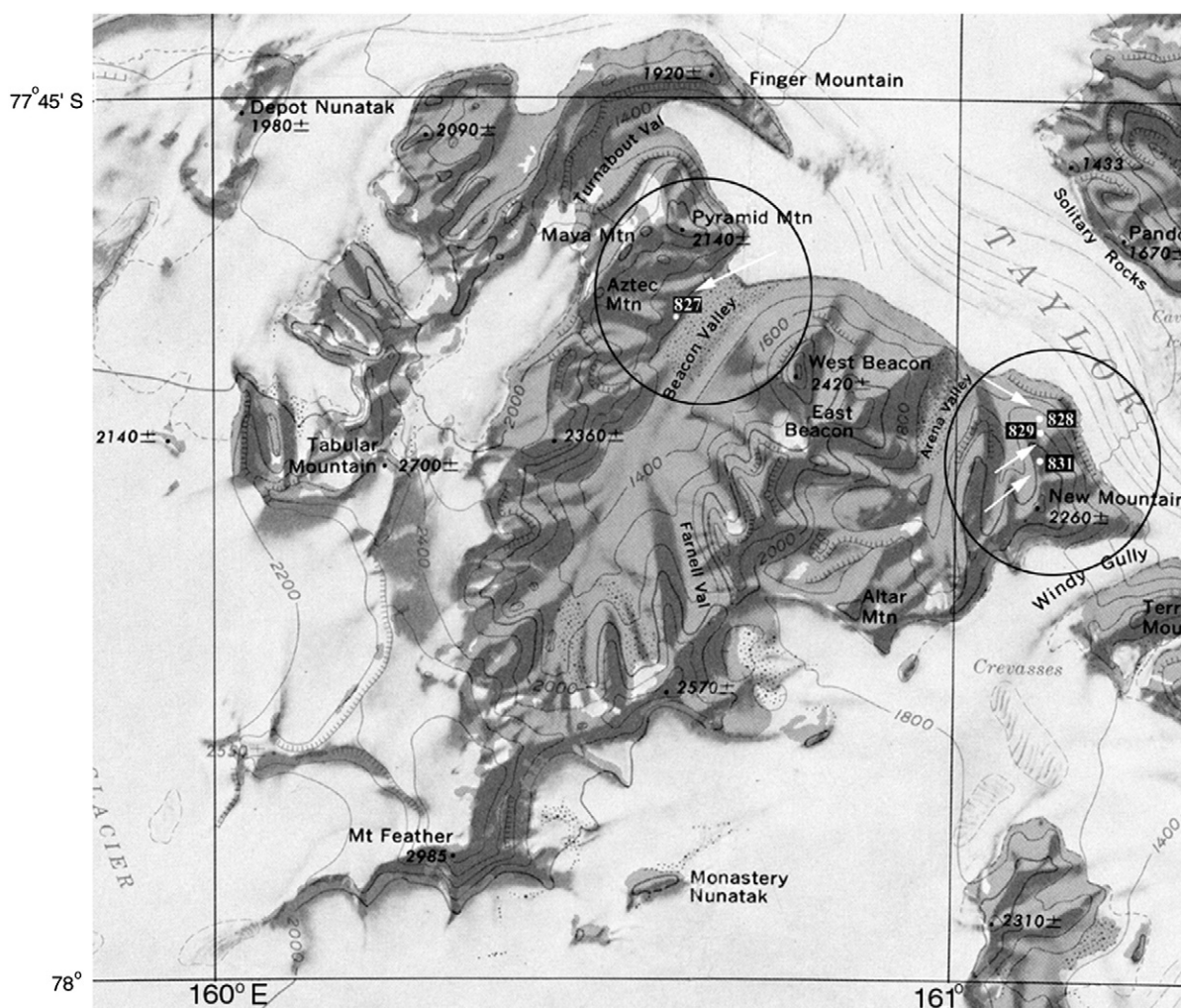
Fig. 1. Location map. Studied sites identified in circled areas.

of bacteria and fungi appear to thrive and proliferate in areas where liquid water exists at least during part of the year or at times in which the climate may have been more hospitable to their growth.

Four sections (location on Fig. 1) in all, two (827 and 831) with single soil profiles each and two (828 and 829) with multi-story profiles are the subject of analysis in this project. Three profiles are dated by relative age dating methods, and one (829) dated by $^{10}$Be (Graham et al., 2002). The latter (Graham et al., 2002) yielded a nitrate inventory age of c.18.5 Ma with upper horizons yielding $^{10}$Be ages of c.15 Ma and the middle layer less than c. 15–17 Ma. These N and $^{10}$Be ages are consistent with the Middle-Miocene transition previously identified by Marchant et al. (1993). Site 827 in the Arena Valley is considered to have an age coeval with sites 828 and 829 on the basis of extractable Fe concentrations (Mahaney et al., 2009), but a precise age placement is not possible. Site 829, with fewer granitic clasts, is considered older than 828, although the two sites are probably separated by little more than 1 or 2 million years, i.e. both sites straddle the Middle-Miocene transition described above. Profile 831 is part of the 'alpine till' group, which is thought to have formed earlier in the Miocene under wet-based conditions, prior to the ingress of outlet glaciers from the Inland Ice Sheet (Hambrey and McKelvey, 2000) that deposited tills at sites 827–829.

Previous XRD analysis (Mahaney et al., 2001) of the samples shown in Fig. 2B confirmed the presence of smectite, illite, and chlorite, all preweathered and transported to sites of emplacement by the inland ice sheet. Recrystallization of clay minerals in the profiles was not expected given the soil microenvironmental constraints, and

no evidence for neoformation of clays was detected, the down profile distribution being detrital. However, the presence of secondary Fe and Al in small concentrations argues for slow rates of oxidation and hydrolysis over long time spans of millions of years affecting all of the minerals shown in Fig. 2B. The main sources of secondary Fe comes from mica, illite, and chlorite; Al from similar sources and feldspar, the majority of which is orthoclase.

Previously Mahaney et al. (2006, 2009) analyzed various forms of secondary Fe and Al with respect to providing relative ages for the profiles at these sites. During the course of these investigations exceedingly small concentrations of pyrophosphate–extractable Al ($Al_p$) were seen to act as a possible proxy for the presence of organically-complexed material, a correlation previously observed in other soil studies (Parfitt and Childs, 1988) and confirmed by XRD and Moessbauer Spectroscopy. Moreover, $Al_p$ concentrations have been shown to correlate well with C and N mobility in Cryosols in Siberia (Mahaney et al., 2010a), in the Rocky Mountains (Mahaney et al., 1999), and in the tropical Andean mountains (Mahaney et al., 2009). While these interrelationships have been well documented in equator to pole positions in both hemispheres, in the Antarctic with near-detection limits for both C and N, trace concentrations of $Al_p$ appear to archive microbes that can be cultured and cultivated, sometimes with prolific growth (Mahaney et al., 2001). To test the reliability of $Al_p$ as a proxy for organically-complexed matter, including the presence of microbes, we took 9 of the 33 samples, selected to represent the median and extreme concentration ranges for C/N, $Al_p$, and DNA quantification. The test for bacterial growth and identification of lipid compounds in the studied
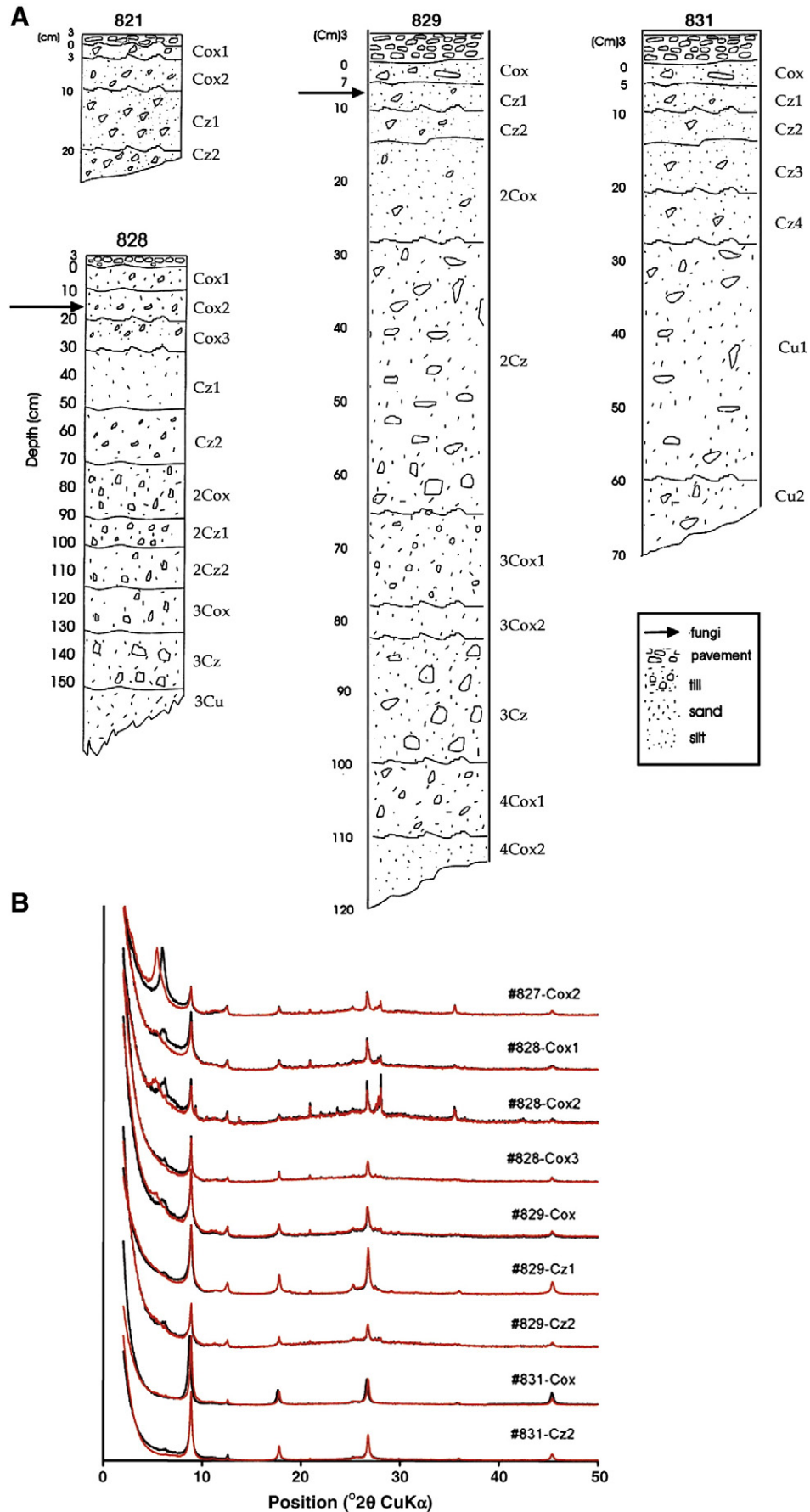
Fig. 2. A, Stratigraphy. Arrows indicate where fungi identified. Exoskeletons of Coelopteran identified in Profile 831-Cz2; B, XRD of Antarctic paleosol horizons.

sample population and their relationship to range in C/N and concentration of $Al_p$ are the subject of this paper. The possibility of identifying and sampling paleosols in Martian ancient terrain might lend itself to the prospect of using secondary Al compounds as indicators of microbial life, either in extant or fossil form.

## 2. Materials and methods

In the Antarctic, sample pits were excavated with shovels and cut back to expose fresh material. The soil descriptions used here are genetic and follow guidelines set out by Mahaney et al. (2009) and differ somewhat from the system of Campbell and Claridge (1987), which was used previously by Mahaney et al. (2001). In the earlier study, horizons were enumerated from A to Z with depth in the profile. In the more recent paper, the usual downward succession of horizons of Fe-rich material over salt-rich material equates to Cox/Cz horizons in the Soil Survey Staff (NSSC, 1995) (Catt, 1990; Birkeland, 1999). Occasionally, where lower concentrations of oxides exist, a C designation (Birkeland, 1999) is invoked. The "ox" designation simply implies the color is stronger than 10YR 5/4 or so (Oyama and Takehara, 1970), a characteristic attributed to more extensive weathering.

Soil color assessments are based on Oyama and Takehara soil chips (1970). At least 500 g samples were collected at the sites to allow for laboratory work, including particle size analysis following the procedures outlined by Day (1965) and geochemical assessment. Samples were wet sieved to separate sands from clay and silt. For the nine samples described here the <2 mm fraction was ground using a McCrone micronising mill, and the resulting slurry freeze-dried to reprecipitate soluble salts before being prepared as a randomly oriented mount. The clay mineralogy was determined on the <2 µm fraction. Following the washing of soluble salts with pure water and the removal of organic matter with $H_2O_2$, as described by Moore and Reynolds (1997), this fraction was extracted by centrifugation. Oriented mounts were prepared by drying the resulting suspension onto glass slides. Ethylene-glycol (EG) solvation of the slides was achieved by exposing them to EG vapor at 70 °C for a minimum of 12 h. XRD patterns were recorded with a Bruker D5000 powder diffractometer equipped with a SolX Si(Li) solid state detector from Baltic Scientific Instruments using $CuK\alpha\_1+2$ radiation. Intensities were recorded at 0.04° 2-theta step intervals from 5 to 80° (6 s counting time per step) and from 2 to 50° (4 s counting time per step) for bulk and clay mineralogy determination, respectively.

Selected sands were subsampled and analyzed under the light microscope, and out of this grain population, a smaller group of samples was subjected to analysis by JEOL-840-JSM Scanning Electron Microscope (SEM) with Energy Dispersive Spectrometry (EDS) using a PGT System at the Department of Geology, University of Toronto, following methods outlined by Mahaney (2002). Photomicrograph and X-ray microanalyses were obtained at accelerating voltages of 10–20 keV and 10–15 keV respectively.

The $Fe_d$ and $Al_d$ extractions were made from 1 g (<2 mm fraction) subsamples, with sodium dithionite, releasing crystalline, amorphous, and organically-bound forms of Fe and Al, as well as sodium citrate buffers, following criteria set out by Coffin (1963). Processed in the dark, acid ammonium oxalate was used to extract ferrihydrite (Parfitt and Childs, 1988) following McKeague and Day (1966). Subsequently, concentrations of Fe and Al were determined using atomic absorption spectrophotometry (AAS). Instrumental neutron activation analysis followed methods identified by Hancock (1984) to extract total Fe and Al in the <2 mm fraction of soil samples.

Data was compiled in Excel spreadsheets that were later exported to Statistica (Statsoft Inc., Tulsa) for more detailed and precise statistical analyses. After this stage, which included cluster analysis, charts were plotted and correlations attempted.

Subsamples of individual surface soil horizons were collected for DNA/bacterial analysis on the basis of color, largely marking Fe release

or salt accumulation in the upper parts of two profiles. Collecting instruments were sterilized, flamed in alcohol prior to bagging. Due to funding constraints, only nine samples were collected for bacterial analysis; sample choices made where expected results might produce positive results. All samples were collected from the profile face, freshly cleaned back and stored in double zip lock bags. Sample bags were opened only at the time of collection, and immediately sealed afterwards.

DNA was extracted from the nine selected samples according to a modified method from Zhou et al. (1996). 5 g of wet sediment was vortexed in the presence of two sterile glass beads and 13.5 ml of DNA extraction buffer (100 mM Tris–HCl [pH 8.0], 100 mM Na-EDTA [pH 8.0], 100 mM $Na_2HSO_4$ [pH 8.0], 1.5 M NaCl, and 1% hexadecylmethylammonium bromide [CTAB]) for 30 s. 100 µl 10 mg/ml proteinase K was then added, and the mixture was incubated on a reciprocating shaker at 37 °C for 30 min at 225 rpm. Following this, 1.5 ml 20% sodium dodecyl sulfate (SDS) was added, and the samples were incubated at 65 °C for 4 h at 100 rpm. Supernatant was transferred to new 50 ml sterile tubes after centrifugation at 6000 g for 10 min at room temperature. The sediment residues were then extracted twice more with 4.5 ml extraction buffer and 500 µl 20% sodium dodecyl sulfate (SDS) at 65 °C for 10 min as before. Combined supernatants were extracted for approximately 5 min with equal volumes of 24:1 (vol/vol) chloroform/isoamyl alcohol. The upper aqueous phase was recovered after centrifugation at 6000 g for 10 min. Crude DNA was precipitated overnight at −20 °C with 0.6 volume isopropanol. The DNA pellet was collected by centrifugation at 15,000 rpm for 20 min and dissolved in minimal volume 1X TE buffer. The crude total DNA was further purified on a 1% low-melting point agarose gel electrophoresis. DNA was purified from the agarose gel by the Illustra gel band purification kit (GE Healthcare, Little Chalfont,

**Table 1**
Selectable extractable and total Fe and Al in selected Antarctic paleosols compared with percent total C. [Data in percent]. The ratio $Al_p/Al_t$ measures downward movement of organically-complexed Al.

| Site | Horizon | Depth (cm) | $Fe_o$ (%) | $Fe_d$ (%) | $Fe_t$ (%) | $Al_p$ (%) | $Al_t$ (%) | $Al_p/Al_t$ | Total C (%) |
|------|---------|-----------|------|------|------|------|------|--------|---------|
| 827 | Cox1 | 0–3 | 0.24 | 0.74 | 6.88 | 0.02 | 4.90 | .004 | >0.01 |
| | Cox2 | 3–10 | 0.28 | 0.81 | 5.85. | 0.03 | 4.30 | .007 | 0.02 |
| | Cz1 | 10–22 | 0.32 | 0.71 | 6.13 | 0.01 | 5.40 | .002 | 0.01 |
| | Cz2 | 22–30 | 0.27 | 0.53 | 6.30 | 0.01 | 4.90 | .002 | <0.01 |
| 828 | Cox1 | 0–10 | 0.97 | 0.95 | 5.98 | 0.02 | 3.90 | .005 | <0.01 |
| | Cox2 | 10–20 | 0.89 | 0.65 | 4.44 | 0.02 | 3.50 | .006 | <0.01 |
| | Cox3 | 20–30 | 0.37 | 0.72 | 4.39 | 0.02 | 3.40 | .006 | <0.01 |
| | Cz1 | 30–51 | 0.42 | 0.50 | 4.25 | 0.01 | 3.50 | .003 | <0.01 |
| | Cz2 | 51–71 | 0.33 | 0.46 | 3.84 | 0.00 | 5.40 | 0 | <0.01 |
| | 2Cox | 71–90 | 0.72 | 0.65 | 4.57 | 0.04 | 4.00 | 0.01 | <0.01 |
| | 2Cz1 | 90–100 | 0.47 | 0.59 | 3.89 | 0.02 | 3.70 | .005 | <0.01 |
| | 2Cz2 | 100–115 | 0.28 | 0.64 | 3.43 | 0.03 | 2.90 | 0.01 | 0.03 |
| | 3Cox | 115–130 | – | – | – | – | -- | | 0.02 |
| | 3Cz | 130–150 | 0.40 | 0.50 | 3.14 | 0.02 | 4.10 | .005 | <0.01 |
| | 3Cu | 150–160 | 0.31 | 0.52 | 3.53 | 0.01 | 3.20 | .003 | 0.04 |
| 829 | Cox | 0–7 | 0.89 | 0.73 | 5.33 | 0.01 | 4.40 | .002 | <0.01 |
| | Cz1 | 7–10 | 0.13 | 0.26 | 1.84 | 0.01 | 4.40 | .002 | 0.03 |
| | Cz2 | 10–16 | 0.91 | 0.72 | 4.96 | 0.00 | 4.50 | 0 | <0.01 |
| | 2Cox | 16–27 | 0.14 | 0.41 | 2.47 | 0.04 | 5.90 | .007 | 0.10 |
| | 2Cz | 27–65 | 0.11 | 0.20 | 1.65 | 0.00 | 2.50 | 0 | 0.34 |
| | 3Cox1 | 65–76 | 0.13 | 0.30 | 2.26 | 0.02 | 4.40 | .005 | 0.18 |
| | 3Cox2 | 76–82 | 0.21 | 0.36 | 2.15 | 0.06 | 2.90 | 0.02 | 0.09 |
| | 3Cz | 82–100 | 0.20 | 0.34 | 2.27 | 0.09 | 4.00 | 0.02 | 0.07 |
| | 4Cox1 | 100–110 | 0.15 | 0.24 | 2.42 | 0.03 | 3.70 | .008 | 0.06 |
| | 4Cox2 | 110–120 | 0.19 | 0.38 | 1.50 | 0.02 | 2.40 | .008 | 0.20 |
| | 4Cz | 120+ | -- | -- | -- | -- | -- | | |
| 831 | Cox | 0–5 | 0.31 | 0.48 | 2.77 | 0.04 | 2.90 | .001 | <0.01 |
| | Cz1 | 5–10 | 0.17 | 0.14 | 0.51 | 0.02 | 1.40 | .143 | <0.01 |
| | Cz2 | 10–14 | 0.10 | 0.16 | 0.50 | 0.15 | 1.80 | .083 | 0.04 |
| | Cz3 | 14–22 | 0.10 | 0.18 | 0.46 | 0.01 | 1.40 | .007 | <0.01 |
| | Cz4 | 22–30 | 0.10 | 0.17 | 0.55 | 0.04 | 1.40 | .029 | 0.01 |
| | Cu1 | 30–60 | 0.06 | 0.04 | 0.33 | 0.01 | 1.10 | .009 | <0.01 |
| | Cu2 | 60+ | | -- | -- | -- | -- | -- | |

-- = not analyzed.

United Kingdom). DNA quantification was determined using an ND-100 Nanodrop Spectrometer (NanoDrop Technologies, Wilmington, DE, USA) with blank and positive controls of ultra-pure water (Sigma-Aldrich p/n W4502) and 20 ng/μl *E.coli* DNA.

## 3. Results

The primary and clay minerals of seven of the nine samples collected for microbial and Fe–Al extract analyses were subjected to XRD (Fig. 2B) to determine variations in mineral composition. Bulk mineralogy was determined for samples 829-Cz1, 829-Cz2, and 831-Cz2. Quartz is the most abundant mineral in all three samples, with labradorite being the most dominant feldspar. A minor occurrence of orthoclase, yet another type of feldspar, is present in samples 829-Cz2

and 831-Cz2. Muscovite was also identified in samples 829-Cz1 and 831-Cz2, whereas diopside was only present in sample 829-Cz2. In addition to these mineral types, soluble salts are abundant with the presence of sulfates (i.e. gypsum in 829-Cz2, gypsum and hexahydrite in 831-Cz2, and Na-sulfate and loweite in 829-Cz1) and nitrates (nitratine and darakpsite in 829-Cz2). A minor amount of calcite was also identified in sample 831-Cz2.

Illite and chlorite are systematically present in the clay-size fraction of all samples in about equivalent proportions as estimated from the relative intensities of their respective diffraction lines. In addition to these two clay phases, smectite is present as a major phase in sample 827-Cox2, and as a minor constituent of samples 828-Cox1, Cox2, and 829-Cox, and as traces in samples 828-Cox3 and 829-Cz2. All three minerals are considered to be preweathered clays that
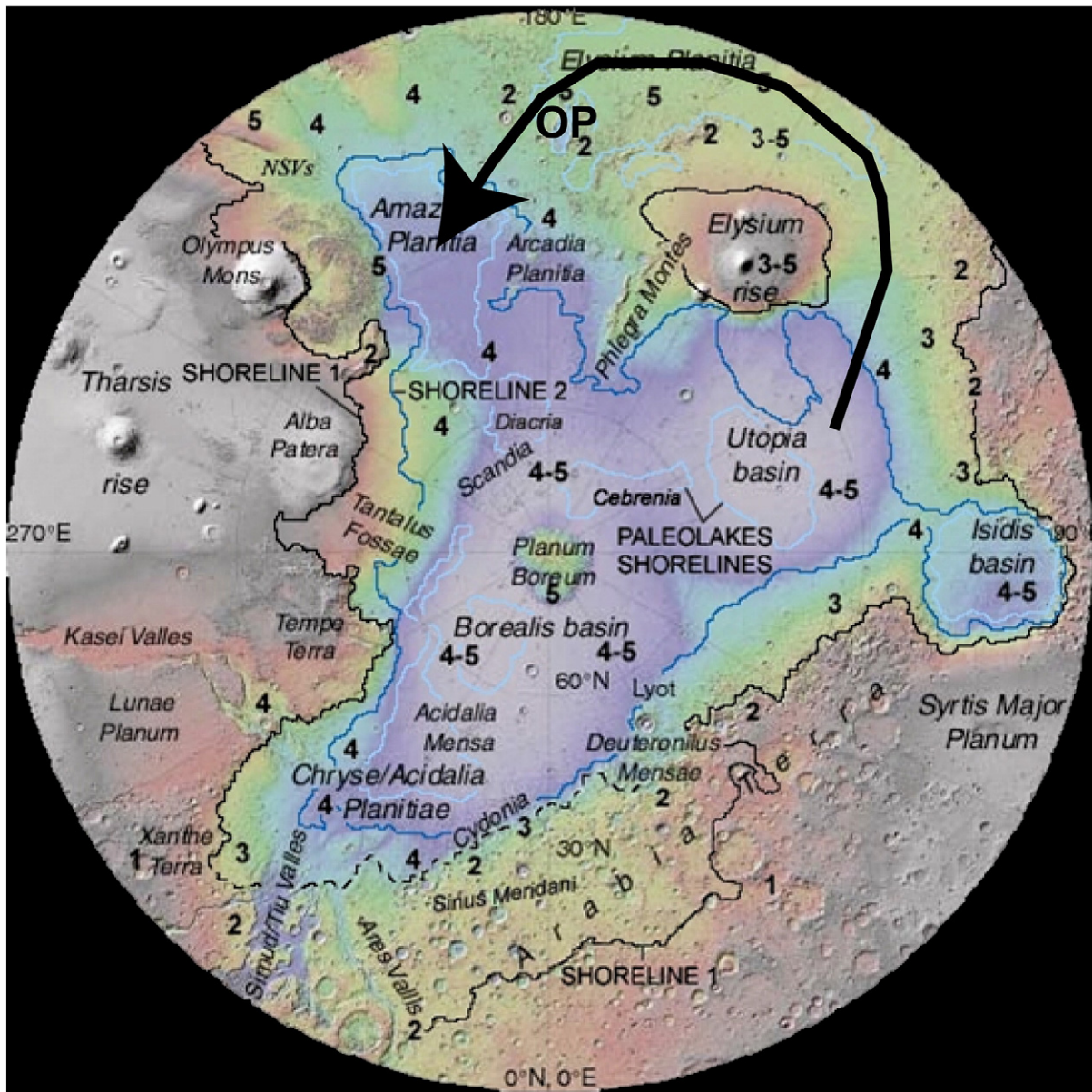


**Fig. 3.** Modified from Fairén et al. (2003), topographic shaded relief map of the northern hemisphere of Mars constructed from Mars Orbiter Laser Altimeter (MOLA) data showing major geographic features of the northern hemisphere, including three major basins (Borealis basin = Vastitas Borealis, Utopia basin = Utopia Planitia, and Isidis basin = Isidis Planitia). Also shown are Shoreline 1 (black line), Contact 1 in Arabia Terra (dashed-black line) and Shoreline 2 (dark blue line). Note that the shorelines of the older and younger oceans have been stable since Mars went into monoplate mode (~3.5 Ga) and weathered under an O-rich atmosphere which is postulated to contain high concentrations of Fe and Al, perhaps on a scale much greater than on Earth. The arrow indicates that an impact into the younger putative ocean ("contact 2") could have generated a tsunami which could have wrapped around Elysium rise, traversing Elysium Planitia, bottle necking south of Orcus Patera to form Marte Vallis, and eventually debouching into Amazonis Planitia. Sediment deposited from tsunami events might have been in contact with the subaerial atmosphere for sufficient time to develop colonies of microbes.

survived transport through the inland ice. The variability of the relative proportions of smectite begs the question as to whether it has any influence on the concentration of organic C or bacterial components, especially since clays such as smectite, a possible sink for water, is pervasive on Mars. The widespread occurrence includes Mawrth Vallis, a potential candidate landing site of the Mars Science Laboratory (MSL; e.g., Bishop et al., 2008) and other parts of the cratered highlands (Mustard et al., 2008; Wray et al., 2009), as well as in the lowlands (Carter et al., 2010). Chloride salts, which provide a habitable environment on Earth, such as in the structurally-controlled basins of the arid Atacama Desert (Davilia et al., 2008), have also been identified widespread in the cratered highlands (Osterloo et al., 2010). Such secondary mineral assemblages point to ancient aqueous activity and mark possible habitable environments on Mars (Dohm, 2011).

Because $Al_p$ trends down profile in other cold temperature locales (Mahaney et al., 1999, 2010a,b) are positive and have been used to measure the degree to which organically-complexed material is translocated from A to B horizons, we decided to test movement in the Antarctic Cryosols. Further, to determine the validity of using $Al_p$ as a proxy for organic C, a test using the distributions of C in four Antarctic Cryosols was measured against known concentrations of $Al_p$. To determine whether Fe was prevalent, the distributions of total Fe and $Fe^{+3}$ extracts were matched horizon by horizon against $Al_p$. Moreover, DNA quantification (μg/g) of selected samples was measured against both C and $Al_p$; the DNA counts were used as a measure for the presence of microorganisms (as DNA released into the soil from dead cells is readily hydrolyzed by nucleases (Thies, 2007)).

Movement of organically-complexed matter can be assessed from Table 1 by matching C against $Al_p$. Of the 33 horizons studied, 12 horizons show a buildup of organic carbon down section, a translocation correlating positively with movement of $Al_p$. The data are approximate only and there are instances where $Al_p$ movement is indicated while organic carbon remains at detection limits. The lack of response in the carbon suite of samples may indicate that $Al_p$ is more sensitive to minute movement of carbon, or that instrumentation used to measure carbon is not accurate at exceedingly low concentrations.

To test the relationship between organic C and $Al_p$, their distributions were subjected to scatterplot analysis to assess the degree to which C correlates with $Al_p$. Despite exceedingly low concentrations of $Al_p$ and organic C, and the presence of occasional outliers, there is a weak correlation of C with $Al_p$. The data in Fig. 4 show that $Al_p$ correlates with very low amounts of C (<0.05% to detection limits). In a few cases, $Al_p$ indicates the presence of C when the LECO Apparatus is at detection limits. The scatter of data shown on Fig. 4A results only in an indirect correlation, the resulting high variability and exceedingly low R factor (Fig. 4B) suggest a tenuous relationship between the two variables.

Selected samples were measured for DNA content with the intent to test the relationship between $Al_p$ and DNA concentrations (Fig. 5). The data indicate considerable variance of DNA with a narrow range of $Al_p$ concentrations with one exception. Given the limited population of data, the results show only that while $Al_p$ targets the presence of biotic components, the latter may fluctuate widely in molecular space.

The presence of Fe necessary for microbe growth and sustenance is sustainable in all horizons, increasing upward in the profiles; the
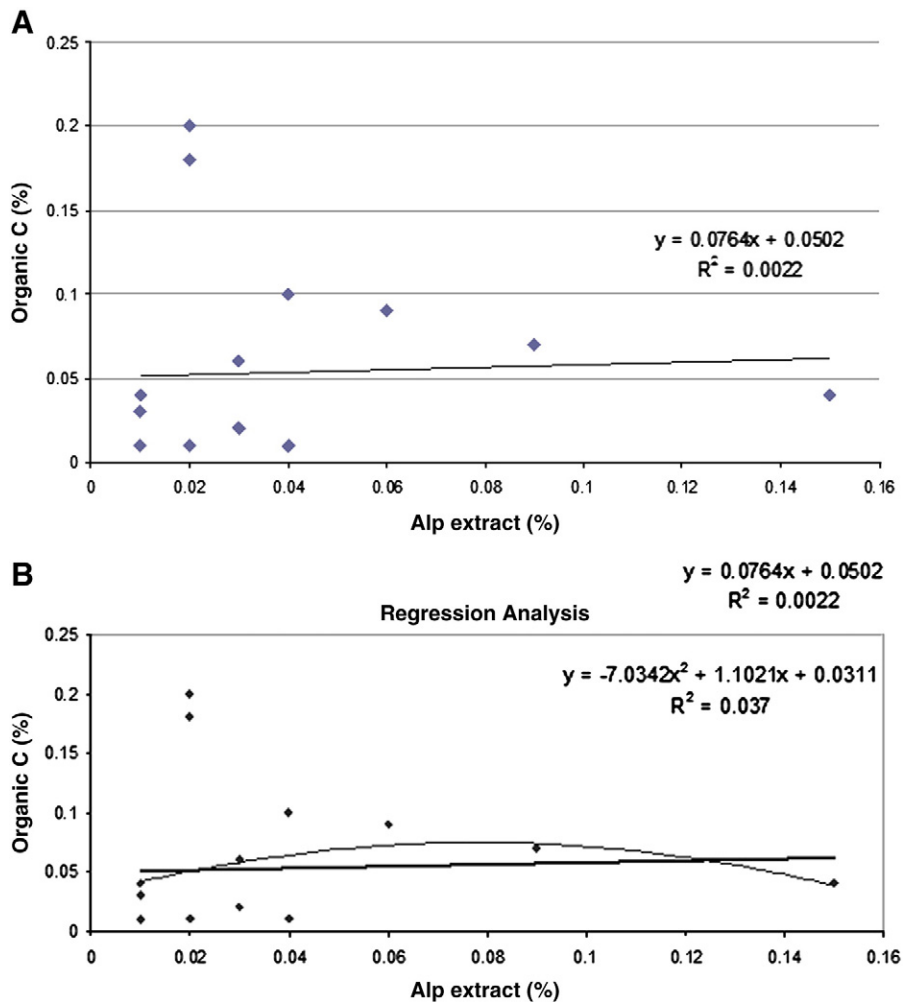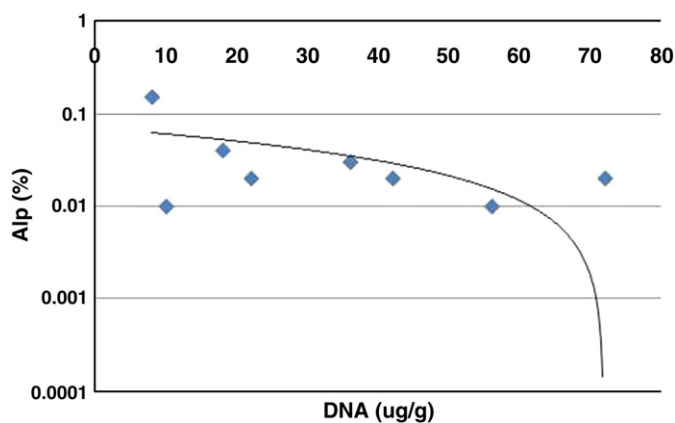


Fig. 4. Scatterplot showing organic C vs. $Al_p$.

**Fig. 5.** Scatterplot showing correlation between DNA and $Al_p$. The data indicate considerable variance of DNA within a narrow concentration range of $Al_p$. Note that $Al_p$ detects organic C when DNA is exceedingly low.

highest concentrations occurring at the surface where sediment has been longest exposed to the subaerial atmosphere. The data (Fig. 6A) depict an increase in $Fe_o$ paralleled by $Fe_d$, except where loss of $Fe_o$ by drainage (rare event) or oxidation over long periods of time have led to the evolution of secondary hematite and goethite, thus increasing the concentration of $Fe_d$. The resulting regression analysis (Fig. 6B) shows a greater correlation between the two variables.

SEM/EDS analysis of grains containing fungi and bacteria in Sections 828, 829, and 831 yielded similar results in terms of Fe and salt coatings with greater variability in salt relative to Fe. The examples shown in Figs. 7 and 8 are representative of what was found in a population of nearly 200 grains, with some samples showing greater weathering effects than what is to be expected in a dry, cold Cryosolic environment. The two ilmenite grains in Fig. 7 exhibit discontinuous coatings of Mg and Ca salts with particularly thicker coatings on
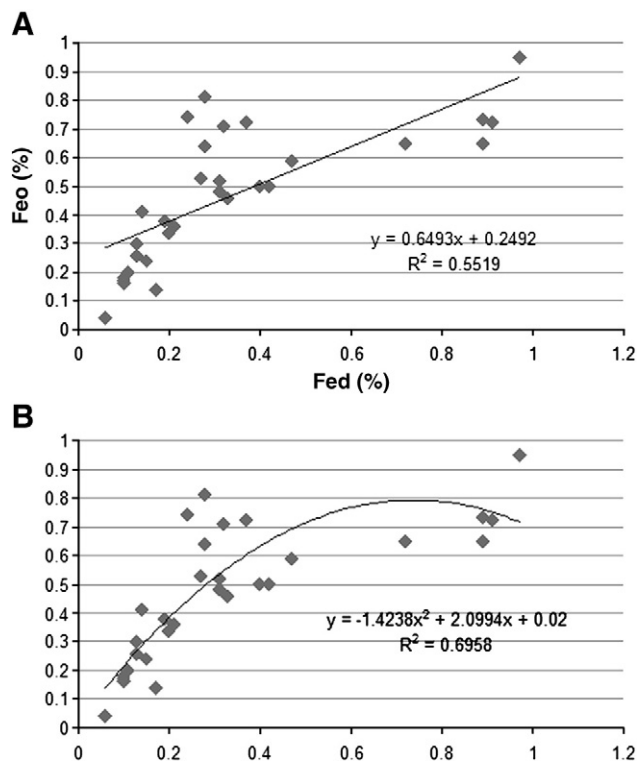


**Fig. 6.** Scatterplot of $Fe_o$ vs. $Fe_d$ showing a positive correlation from less weathered to more strongly weathered horizons within the pedostratigraphic profiles in the Antarctic Dry Valleys.

adhering particles. In places, Fe coatings are common but salts dominate across much of the grain surfaces. The round spindle-shaped pyroxene grain in Fig. 8A and scattered v-shaped percussion cracks indicate tumbling, perhaps in meltwater prior to the wet/cold ice base transition of ~20 Ma (Marchant et al., 1993). Enlargement of the pyroxene surface shows an etched surface with v-shaped percussion cracks, etching seemingly following crystallographic planes. Taking the lighter fringes as possibly demarcating Fe, arguably suggests that secondary Fe development follows etching/corrosion of the grain surface. Quartz, on the other hand, carries infrequent, thin coatings of Fe and salts.

## 4. Implications for Mars

Gamma Ray Spectrometer (GRS)-based research on Mars indicates elevated Fe concentrations in distinct regions below the putative Noachian paleoocean demarcations (Parker et al., 1993), which include areas associated with debouchment regions of the circum-Chryse outflow channel system (Dohm et al., 2008a). The ocean shore demarcation has been proposed based on geomorphology and topography (e.g., Fig. 3), possibly marking marine limits that would cover one third of the planet's surface (Fairén et al., 2003; Mahaney et al., 2010b), an area equivalent to the Mediterranean Basin on Earth. The Noachian Period of Mars is the oldest geologic period, one that records dynamic geologic activity and relatively high erosion rates, which includes possible plate tectonism during the incipient development of the planet, a magnetosphere, and relatively thick atmosphere with a composition similar to Earth (Baker et al., 2007). The Martian environment had the potential to foster soil evolution over long periods of time, long enough to produce copious paleosols, perhaps much older than on Earth. The period of high erosion resulted in the formation of valley networks, alluvial fans, and layered sedimentary deposits (Baker et al., 2007); the latter, if stable for long periods, may archive the ancient environmental history of the planet. This compares with later stagnant-lid activity, which includes the development of the Tharsis magmatic complex, also referred to as the Tharsis Superplume (Dohm et al., 2007). Tharsis appears to have formed in at least five major stages, which include magmatic-driven flooding, ponding in the northern plains to form water bodies ranging from lakes to oceans, and transient climatic perturbations (Scott et al., 1995; Dohm and Tanaka, 1999; Baker, 2001; Fairén et al., 2003; Dohm et al., 2001, 2007, 2008a,b). Such activity, which may have contributed significantly to the formation of sulfates (Fan et al., 2008), cannot be ruled out in the future (Dohm et al., 2008b).

The Early and Middle Noachian epochs of Mars may have had sufficient oxygen (Baker et al., 2007), as well as a protective magnetosphere (Zuber, 2001), conducive to the generation and evolution of primitive life. With Fe concentrations observed through the GRS instrument, which detects elemental concentrations in rock materials at depths up to ~0.3 m (Boynton et al., 2007), such as below the putative Noachian shoreline demarcation (Dohm et al., 2008a) (Fig. 3), we estimate the genesis of $Fe^{+3}$ by comparison with known concentrations of secondary Fe in the Antarctic paleosols. To achieve this, it is necessary to normalize temperatures between the two and to account for both differences in $Fe^{+2}$ and a shortened phase of oxidation weathering on Earth compared to a more expanded time period on Mars (<20 Ma on Earth vs. 500 Ma to 1 Ga or more on Mars). Using Earth concentrations of Fe in the Antarctic as a standard, and assuming the Fe took $15 \times 10^6$ yr to form, the expected $Fe^{+3}$ on Mars would be 50 to 100 times greater, and greater again if dating back to the Noachian/ Hesperian transition (roughly 3.6 Gy (Hartmann and Neukum, 2001), realizing that the estimated absolute age may be significantly in error).

There is also the need to address the disparity in total Fe between Earth and Mars. Mean totals for $Fe_2O_3$ on Mars range between 15 and 19% (Bertka and Fei, 1998; Bell et al., 2000), which suggest oxidation on Mars could be one of the major weathering processes (Mahaney et al., 2001), and with a reasonable redox potential on Mars, may well have produced paleosols with sufficient $Fe^{+3}$ to satisfy the physiological
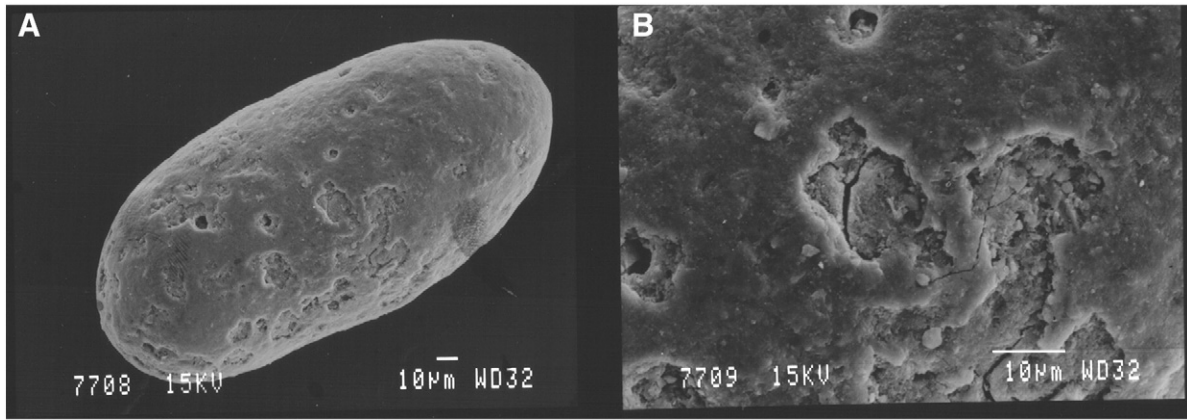
**Fig. 7.** Spindle-shaped pyroxene with craters of unknown origin, minor v-shaped percussion cracks that could relate to turbulence in meltwater and partial etched surface. This could be a reworked grain from prior to the wet/cold transition (Early Miocene) or older.

requirements of microbes, provided liquid water was available. If, Archaea, bacteria, fungi, and protists were to grow and proliferate in these paleosols, they surely would have left an organic residue archived in the weathered sediment record just as in the Dry Valley paleosols.

The primary objective of this work is to estimate the probability for the development of microbial life on Mars using known concentrations of two essential ingredients on Earth, $H_2O$ and Fe, in Mars-analogue environments such as Antarctica. A further question is to compare variable extracts of Fe with Al, for while some forms of Fe are known to be soluble, Al under normal terrestrial pH of 4.0 to 8.0 is insoluble; Al is often used as a standard with which to measure the downward movement of more soluble materials such as alkaline Earths and alkali metals weathering out of plagioclase and associated minerals (Mahaney et al., 1999). Whereas the knowledge of the distribution of Al on Mars is still in a formative stage, it is likely that the GRS data, when released, will provide an estimate of total Al that can be compared with the Antarctic data. While estimations of secondary forms of Al might be nearly impossible to estimate, this would provide a necessary base line data on the genesis of various species of clay minerals required for amino acid transport from oceans to land, an essential factor for the further evolution of life. For clay mineral recrystallization to proceed, pH in high alkaline and acidic environments would have to equilibrate down to between pH 4 and 8 (Black, 1967).

Because the concentration of total Fe on Mars is about 4.5 times that of Earth (Bell et al., 2000), it is expected that secondary Fe

concentrations in Noachian (as per above, roughly >3.6 Ga) outcrops/ paleosols on Mars might be considerably higher when compared with similar cold-climate locales on Earth. If so, then the total $Fe^{+3}$ would be orders of magnitude in excess of 50 to 100 times.

## 5. Discussion

The bulk (<2 mm fraction) and clay mineral (<2 μm) compositions depict a relationship to dolerite, granite, and sandstone lithologies that make up the clast and matrix composition of all tills in the area. The one dominant clay mineral is smectite that shows a high variability, being present as a major clay phase only at Aztec Mountain (sample 827) and exhibiting lower concentrations in two of the samples at site locations 828 and 829. It should be noted (Fig. 5) that organic carbon remains low in sample 827 with high smectite while DNA was on the high side, thus suggesting that bacteria might be attracted to smectite, possibly because of its flexible lattice and adsorbed water content (minor content and dry frozen most of the year), though more sampling and laboratory analyses are necessary to test this hypothesis.

Pyrophosphate-extractable Al appears to adsorb organically-complexed matter and thus acts as a proxy for the presence of organic compounds including organic carbon and DNA. The correlation with organic carbon is stronger as indicated from the scatterplot shown in Fig. 4A. What is unexpected from this correlation is that $Al_p$ can target the presence of minute organic compounds when organic
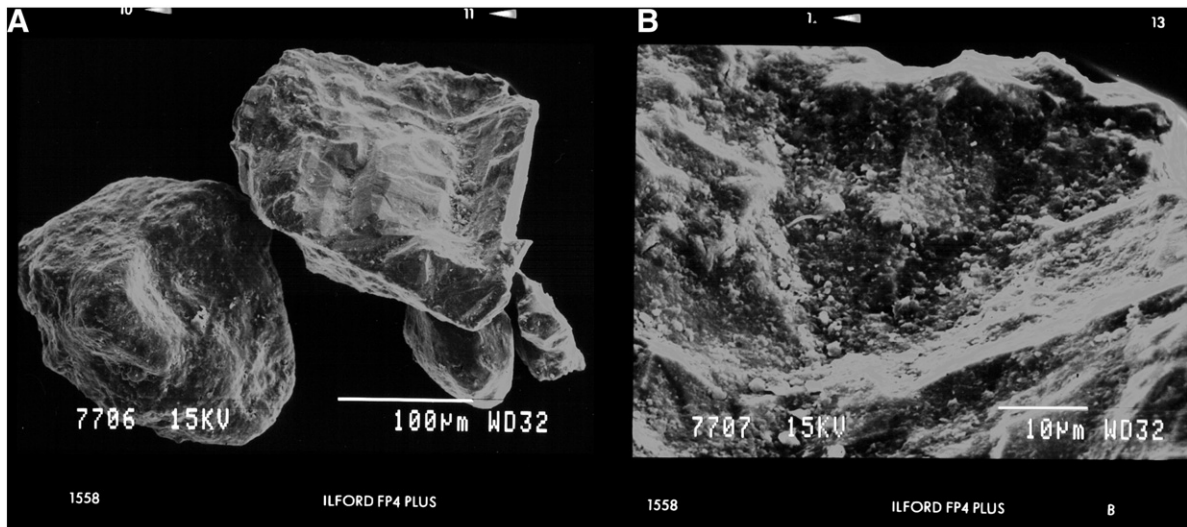


**Fig. 8.** Two angular and subangular ilmenite grains with adhering particles in 828-Cox2. Coatings of $CaSO_4 2H_2O$ and $MgSO_4$. Ca:Mg ratios are 1.8:1.0 overall.

C is at detection limits, a correlation that is exceedingly useful for studies where organic matter is at very low concentration. This makes the extraction method useful in studies where the minute detection of organics helps to shed light on other environmental processes such as presence of bacteria/fungi, fluctuation of redox potential, translocation of organics in active or even inactive pedogenic systems, and relation to certain types of vegetation (conifers to deciduous species; Birkeland, 1999).

Three methods have been used over the last half century to extract Fe and Al from a number of different soil taxa. These three extractions used Na-pyrophosphate (p), acid ammonium oxalate (o), and Na-dithionite-citrate (d), each reagent considered to extract different forms of Fe and Al (Alexander, 1974; McKeague and Day (1966)). Using Moessbauer methods, Parfitt and Childs (1988) showed that $Fe_p$ could not be used to measure organically-complexed Fe. Additional XRD investigations by Mahaney et al. (1999) showed the $Fe_p$ extract contained appreciable concentrations of crystalline Fe oxides However, $Al_p$ was shown to relate to Al in humus complexes; it can be used with confidence to estimate Al in organic complexes (Parfitt and Childs, 1988). Moreover, the ratio $Al_p/Al_t$ has proved particularly useful in assessing translocation in cold mountain soils and Cryosols (Mahaney et al., 2006, 2009, 2010a).

Overall, the compositional variation and concentrations of secondary oxides/coatings in <2 mm matrix material in tills from Early to Middle Miocene paleosols in the Antarctic Dry Valleys (Mahaney et al., 2001, 2009) provide putative evidence for microbial life. The paleosols date to between 15 and 18 Ma by $^{10}Be$, forming prior to and just following the transition from warm-based to cold-based ice, when the climate is thought to have entered a prolonged cold/dry period in which soil moisture was non-existent for most of the year; cf. to postulated climatic changes on Mars which may have had a similar effect. Each pedostratigraphic succession studied consists of a thin pebble bed in which fines have been deflated with clasts carrying a long ventifact history evidenced by minor corrosion/etching on downwind aspects, presumably derived from short-lived periods of snow melt which hydrolyzed mineral surfaces producing a pitted/etched surface. These pebble beds, underlain by horizon(s) of sandy silty material, carry appreciable coatings of secondary Fe, which, in turn, are underlain with salt-enriched materials of sufficient concentration to insure water remains in a liquid state down to 243 K (Fairén et al., 2009). Each buried paleosol in succession took a million plus years to form, the uppermost paleosol remaining in contact with the subaerial atmosphere for ca. 15 Ma. (Mahaney et al., 2009). The entire paleosol stack in each case has been dry frozen for most of its existence, only occasionally interrupted by the ingress of liquid moisture from occasional summer snow melt (which in the last decade has become more frequent due to global warming). The Antarctic paleosols as described above are close correlatives to what one may expect on Mars (Mahaney et al., 2001).

The progressive release of secondary Fe and Al oxides shows variable percentages of individual oxihydrites relative to chemical element totals. To consume total Fe and Al would require tens of millions of additional years. The slow progression of $Fe_d/Fe_t$ (Na-dithionite extractable Fe/total Fe; see Mahaney et al., 1999), used as a measure of relative age in other warmer alpine and Arctic climates, was interpreted by Mahaney et al. (2009) to amount to <15% of the total Fe available for weathering. The sum total of $Fe_d$ (goethite + hematite + ferrihydrite) as secondary weathering products increases as $Fe^{+2}$ is converted to $Fe^{+3}$ over time. Ferrihydrite ($Fe_{10}O_{15} \cdot 9H_2O$) variability in these Antarctic paleosols may indicate the presence of fluctuating/ perched ground water tables, further suggesting that liquid water accumulated in mid-profile in some instances, albeit with unknown concentrations, perhaps during periods when the climate was somewhat warmer for several weeks during the summer. In fact, increased $Fe_o$ in certain horizons might relate to Holocene vs. full glacial Pleistocene climates with somewhat increased melting occurring over the last 10 kyr.

Variable Fe and Al ratios and arithmetic functions argue for extremely slow but sustainable release of oxides in a cold, polar desert climate in which temperatures prohibit the formation of clay minerals (Mahaney et al., 2001), but chemistry dictates a high probability of microbial life. The presence of detrital distribution of secondary clay mineral species likely amounts to residue from pre-Miocene climates and glacial transport from source areas more conducive to clay mineral genesis and aerosolic input over time. A similar process might be postulated for Mars, although with a higher proportion of 2:1 (Si: Al) clays that might be expected to carry adsorbed amino acids and possibly microbes.

Other extracts including $Al_o$ and $Al_d$ (data not included here) should be used with caution since most workers (Birkeland et al., 1989; Mahaney et al., 1999, 2010a) consider the $Al_o$ extracts to measure more than amorphous Al; also, $Al_d$ usually has lower concentrations probably because Na-dithionite does not extract all secondary crystalline Al. While both extracts increase with time, the relation between the two is unknown, and while often recorded, the exact concentration of amorphous to crystalline forms is unknown. The $Fe_o$ and $Fe_d$ data shown in Table 1 provide proxy data of ferrihydrite ($Fe_o \times 1.7$) and $Fe_d$ trends which support the discontinuous presence of bacteria, both forms of Fe needed for respiration.

Taken against $Fe_t$ in the Antarctic paleosols, approximately 1/6 or less of the $Fe^{+2}$ has been converted to $Fe^{+3}$ in ~15 my, an estimation of just how slow the oxidation process is in the dry frozen soils of the Antarctic Dry Valleys. Dithionite-citrate reagent dissolves goethite and hematite as well as ferrihydrite. Quantitative estimates of goethite and hematite can be made using $Fe_d-Fe_o$, which with the samples discussed herein show mixed ratios of the amount of goethite plus hematite present. Where $Fe_o$ is slightly higher than $Fe_d$ in a few samples, the presence of magnetite might be at fault (Walker, 1981), or possibly variable concentrations of Fe were present in the two separate subsamples weighed for analyses.

DNA was extracted directly from soils to give as close a representation of the current bacterial content as possible for each selected paleosol. This was done because of the limitations experienced when attempting to grow extant bacteria from a sample in the limited confines of the laboratory. This is an important consideration as traditional culturing methods may preferentially encourage the growth of low numbering species due to the altered conditions and hence provide a false overview of the biologic samples. Different growth conditions such as substrate, pH, nutrients, electron donor/acceptors, and temperature (to name but a few) may produce widely varying DNA concentrations. Therefore, it was considered to be prudent to rely on a more direct DNA quantification method. It is possible that the relatively higher levels of organic carbon resident within these particular soils supported a limited ecosystem or represent the organisms themselves in an abundance high enough to be detected (using the methods outlined above). We suggest that based upon $Al_p$ and organic C studies, the total DNA from the paleosols (Table 2) should be subjected to a highly sensitive quantitative technique such as quantitative PCR, as this would be an extremely useful biological indicator of life in such hostile locations such as the Antarctic and possibly the Martian lithosphere.

**Table 2**
Total DNA and $Al_p$ concentrations in selected Antarctic paleosol horizons.

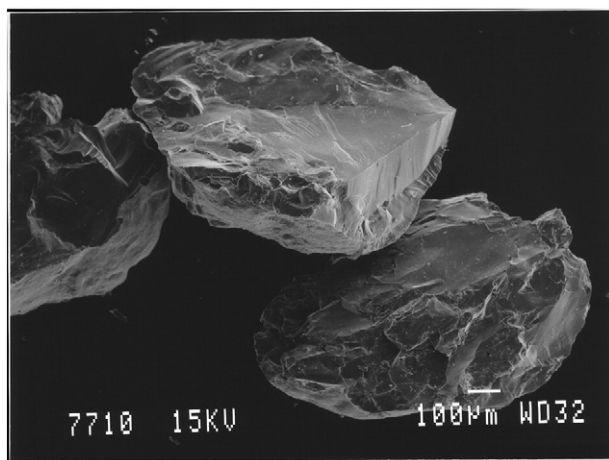| Site | Horizon | DNA (μg/g) | $Al_p$ |
|------|---------|------------|--------|
| 827 | Cox2 | 36 | 0.03 |
| 828 | Cox1 | 72 | 0.02 |
| | Cox2 | 42 | 0.02 |
| | Cox3 | 22 | 0.02 |
| 829 | Cox | 10 | 0.01 |
| | Cz1 | 56 | 0.01 |
| | Cz2 | 31 | 0.00 |
| 831 | Cox | 18 | 0.04 |
| | Cz2 | 8 | 0.15 |

**Fig. 9.** Three angular, glacially-crushed quartz grains with sharp edges, deep grooves, some adhering particles and multiple fractures. The grain to left is partially coated (bottom) with Fe and $CaSO_4$.

The weathering data in Figs. 7 and 8 suggest variable corrosion/hydrolysis of Fe-rich minerals in the upper horizons of profiles with some showing greater salt content than others. Still other grains such as the pyroxene in Fig. 7A and B indicate possible preweathered effects that occurred prior to the wet/cold based ice transition of the Early Miocene or earlier. Both pyroxene and ilmenite might be expected to weather at about the same intensity assuming the same weathering microenvironment across the horizon which further strengthens the argument for inherited preweathered characteristics in some instances. The possibility that salt tends to maintain water in a liquid form to near $-50\ °C$, a condition favoring corrosion/hydrolysis and oxidation in Fe-rich grains, is further substantiated by analysis of quartz with discontinuous salt coatings and minor secondary Fe oxide coats (Fig. 9). The population of data is not significant enough to argue for more than a tenuous correlation, but data collected so far leads toward a postulation that salt and secondary Fe encrustations form more rapidly on Fe-rich grains than on felsic minerals.

Future investigations that involve a search for extant or fossil life on Mars may well rely on the analysis of Al extracts, which have been shown here to be proxy indicators of minute amounts of organic carbon and DNA. If life is detected on the Red Planet, it will likely be found in paleosols, presumably salt and Fe-rich pedons similar to what exist in the Antarctic Dry Valleys. Because Fe and salts are detected to occur at and near the surface of Mars, possibly together in significant concentrations, the presence of life, if existing, may well hinge on the presence of mineralic soils of like kind to those in Antarctica. Moreover, $Al_p$ may be used to detect living microbes (or their former existence) when normal instrumentation fails to signal the presence of organic carbon, since concentrations of organic carbon in Cryosols, as outlined in this study, often amount to a minute residue of fossil/live microbes.

## 6. Conclusion

The data presented and discussed herein point to the value of studying micro components resident in paleosols in ancient landforms with the objective of gaining new information on the relationship between abiotic and biotic components that shed light on age assessments and paleoenvironmental conditions. As paleosols are likely to be prevalent on Mars, continued investigation of Earth counterparts, such as those in the Antarctic, offers the prospect of helping to unravel the geochemical and environmental histories, as well as life-habitability potential of the red planet.

The relationship of $Al_p$ with % C suggests that pyrophosphate extractable Al corresponds to Al in humus complexes. Unlike previous estimates of this correlation, the analysis carried out herein was completed at exceedingly low concentration of both the Al extract and organic carbon. Furthermore, $Al_p$ can be used as an important analytical tool in carbon-starved environments to detect minute amounts of organic material when normal biotic analytical systems are at or very close to detection limits. This is substantiated where bacteria have been cultured in samples with very low concentrations of both $Al_p$ and organic C. The use of $Al_p$, as a biomarker, rivals the detection of cold polar desert ancient and modern biomarkers (Wynn-Williams et al., 2000), serving as a candidate bioindicator for the future exploration of extant or fossil life Mars. Such a biomarker may be useful in testing the hypothesis of whether life exits beyond Earth, such as in Fe- and salt-enriched paleosols that may record a dynamic geologic and hydrologic Martian past, especially during the early stages of development of the red planet, as evidenced by geomorphic, geologic, and geophysical information (Zuber, 2001; Baker et al., 2007; Fairén et al., 2010).

The limited test of DNA vs. $Al_p$ shows that concentrations of $Al_p$ show little variance as DNA fluctuates across a wide concentration of 8 to 72 μg/g. The correlation of increased DNA to organic carbon in some paleosols, no matter how tentative, is an interesting biological indicator worthy of further research using different enrichment conditions or more appropriately total DNA extraction and subsequent quantitative PCR.

## References

Alexander, E.B., 1974. Extractable iron in relation to soil age on terraces along the Truckee River, Nevada. Soil Science Society of America Proceedings 38, 121–124.
Baker, V.R., 2001. Water and the Martian landscape. Nature 412, 228–236.
Baker, V.R., Maruyama, S., Dohm, J.M., 2007. Tharsis superplume and the geological evolution of early Mars. In: Yuen, D.A., Maruyama, S., Karato, S.-I., Windley, B.F. (Eds.), Superplumes: Beyond Plate Tectonics. Springer, pp. 507–523.
Bell III, J.F., McSween, H.Y., Crisp, J.A., Morris, R.V., Moore, H.J., Ghosh, A., Bishop, J.L., Anderson, R.C., Bruckner, J., Economou, T., Greenwood, J.P., Gunnlagsson, H.P., Hargraves, R.M., Hviid, S., Knudsen, J.M., Madsen, M.B., Reid, R., Rieder, R., Soderblom, L., 2000. Mineralogic and compositional properties of Martian soil and dust: results from Mars Pathfinder. Journal of Geophysical Research 105, 1721–1755.
Bertka, C.M., Fei, Y., 1998. Implications of Pathfinder data for the bulk iron content of mars. Lunar Planet. Sci. Conf. XXVIIII, #1252 (abstract) [CD-ROM].
Birkeland, P.W., 1999. Soils and Geomorphology. Oxford University Press, Oxford, U.K. 430 pp.
Birkeland, P.W., Burke, R.M., Benedict, J.B., 1989. Pedogenic gradients for Fe and Al accumulation and P depletion in arctic and alpine soils as a function of time and climate. Quaternary Research 32, 193–204.
Bishop, J.L., Noe Dobrea, E.Z., Mckeown, N.K., Parente, M., Ehlmann, B.L., Michalski, J.R., Milliken, R.E., Poulet, F., Swayze, G.A., Mustard, J.F., Murchie, S.L., Bibring, J.-P., 2008. Phyllosilicate diversity and past aqueous activity revealed at Mawrth Vallis, Mars. Science 321, 830–833.
Black, A.B., 1967. Applications, electrokinetic characteristics of hydrous oxides of aluminum and iron. In: Faust, S.D., Hunter, J.V. (Eds.), Principles and Applications of Water Chemistry. John Wiley and Sons, NY, pp. 247–300.
Boynton, W.V., Taylor, G.J., Evans, L.G., Reedy, R.C., Starr, R., Janes, D.M., Kerry, K.E., Drake, D.M., Kim, K.J., Williams, R.M.S., Crombie, M.K., Dohm, J.M., Baker, V., Metzger, A.E., Karunatillake, S., Keller, J.M., Newsom, H.E., Arnold, J.R., Brückner, J., Englert, P.A.J., Gasnault, O., Sprague, A.L., Mitrofanov, I., Squyres, S.W., Trombka, J.I., d'Uston, L., Wänke, H., Hamara, D.K., 2007. Concentration of H, Si, Cl, K, Fe, and Th in the low- and mid-latitude regions of Mars. Journal of Geophysical Research 112, E12S99. doi:10.1029/2007JE002887.
Campbell, I.B., Claridge, G.G.C., 1987. Antarctica: Soils, Weathering Processes and Environment. Elsevier, Amsterdam. 368 pp.
Carter, J., Poulet, E., Bibring, J.-P., Murchie, S., 2010. Detection of hydrated silicates in crustal outcrops on the northern plains of Mars. Science 328, 1682–1684.
Catt, J.A. (Ed.), 1990. Palaeopedology Manual: Quaternary International, 6, pp. 1–95.

Claridge, G.G.C., 1977. The salts in Antarctic soils, their distribution and relationship to soil processes. Soil Science 123, 377–384.

Claridge, G.G.C., Campbell, I.B., 1968. Origin of nitrate deposits. Nature 217, 428–430.

Coffin, D.E., 1963. A method for the determination of free iron in soils and clays. Canadian Journal of Soil Science 43, 7–17.

Davilia, A.F., Gomez-Silva, A., Ascaso, C., Olivares, H., McKay, C.P., Wierzchos, J., 2008. Facilitation of endolithic microbial survival in the Atacama Desert by mineral deliquescence. Journal of Geophysical Research 113, 1028–1037.

Day, P.E., 1965. Particle fractionation and particle size analysis. In: Black, C.A. (Ed.), Methods of Soil Analysis. American Society of Agronomy, Madison, Wisconsin, pp. 545–567.

Dohm, J.M., 2011. Inventory of potentially habitable environments on Mars. Lunar Planet. Sci. Conf., XXXXII, #2234 (abstract) (CD-ROM).

Dohm, J.M., Tanaka, K., 1999. Geology of the Thaumasia Region, Mars: plateau development, valley origins, and magmatic evolution. Planetary and Space Science 47, 411–431.

Dohm, J.M., Ferris, J.C., Baker, V.R., Anderson, R.C., Hare, T.M., Strom, R.G., Barlow, N.G., Tanaka, K.L., Klemaszewski, J.E., Scott, D.H., 2001. Ancient drainage basin of the Tharsis region, Mars: potential source for outflow channel systems and putative oceans or paleolakes. Journal of Geophysical Research 106, 32943–32958.

Dohm, J.M., Baker, V.R., Maruyama, S., Anderson, R.C., 2007. Traits and evolution of the Tharsis superplume, Mars. In: Yuen, D.A., Maruyama, S., Karato, S.-I., Windley, B.F. (Eds.), Superplumes: Beyond Plate Tectonics. Springer, pp. 523–537.

Dohm, J.M., Anderson, R.C., Barlow, N.G., Miyamoto, H., Davies, A.G., Taylor, G.J., Baker, V.R., Boynton, W.V., Keller, J., Kerry, K., Janes, D., Fairén, A.G., Schulze-Makuch, D., Glamoclija, M., Marinangeli, L., Ori, G.G., Strom, R.G., Williams, J.-P., Ferris, J.C., Rodríguez, J.A.P., de Pablo, M.A., Karunatillake, S., 2008a. Recent geological and hydrological activity on Mars: the Tharsis/Elysium corridor. Planetary and Space Science 56, 985–1013.

Dohm, J.M., et al., 2008b. GRS evidence and the possibility of ancient oceans on Mars. Special Planet. & Space Sci. doi:10.1016/j.pss.2008.10.008 Issue: Mars Analogues-G Ori et al.

Fairén, A.G., Dohm, J.M., Baker, V.R., de Pablo, M.A., Ruiz, J., Ferris, J.C., Anderson, R.C., 2003. Episodic flood inundations of the northern plains of Mars. Icarus 165, 53–67.

Fairén, A.G., Davila, A.F., Gago-Duport, L., Amils, R., McKay, P., 2009. Stability against freezing of aqueous solutions on early Mars. Nature 459, 401–404.

Fairén, A.G., Davila, A.F., Lim, D., Bramall, N., Bonaccorsi, R., Zavaleta, J., Uceda, E.R., Stoker, C., Wierzchos, J., Dohm, J.M., Amils, R., Andersen, D., McKay, C.P., 2010. Astrobiology through the ages of Mars: the study of terrestrial analogues to understand the habitability of Mars. Astrobiology 10, 821–843.

Falkowski, P.G., Fenchel, T., Delong, E.F., 2008. The microbial engines that drives Earth's biogeochemical cycles. Science 320 (5879), 1034–1039.

Fan, C., Schulze-Makuch, D., Fairén, A.G., Wolff, J.A., 2008. A new hypothesis for the origin and redistribution of sulfates in the equatorial region of western Mars. Geophysical Research Letters 35, L06201. doi:10.1029/2007GL033079.

Graham, I.J., Ditchburn, R.G., Claridge, G.G.C., Sheppard, D.S., Whitehead, N.E., Xondervan, A., Sheppard, D.S., 2002. Dating Antarctic soils using atmosphere-derived [10]Be and nitrate. In: Gamble, J.A., Skinner, D.N.B., Henry, S. (Eds.), Antarctica at the Close of a Millennium: Proc. 8th Int. Symposium on Antarctic Earth Sciences, pp. 429–436.

Hambrey, M.J., McKelvey, B., 2000. Major Neogene fluctuations of the East Antarctic ice sheet: stratigraphic evidence from the Lambert Glacier region. Geology 28, 865–960.

Hancock, R.G.V., 1984. On the source of clay used for Cologne Roman pottery. Archaeometry 26, 210–217.

Hartmann, W.K., Neukum, G., 2001. Cratering chronology and the evolution of Mars. Space Science Reviews 96, 165–194.

Mahaney, W.C., 2002. Atlas of Sand Grain Surface Textures and Applications. Oxford University Press, Oxford, UK. 237 pp.

Mahaney, W.C., Sanmugadas, K., Hancock, R.G.V., 1999. Extractable Fe and Al of soils in the Middle Teton chronosequence, western Wyoming, U.S.A. Zeitschrift für Geomorphologie 43, 393–407.

Mahaney, W.C., Malloch, D., Hancock, R.G.V., Campbell, I.B., Sheppard, D., 2000. Microbiology and geochemistry of Antarctic paleosols. Second International Conference on Mars Polar Science and Exploration, Reykjavik, Iceland, p. 113. Aug., 21–25.

Mahaney, W.C., Dohm, J.M., Baker, V.R., Newsom, H.E., Malloch, D., Hancock, R.G.V., Campbell, I., Sheppard, D., Milner, M.W., 2001. Morphogenesis of Antarctic paleosols: martian analogue. Icarus 154, 113–130.

Mahaney, W.C., Falen, A.L., Fosberg, M.A., Hancock, R.G.V., 2006. Later Pleistocene and Holocene soils in Mammoth Basin and Green River areas, Wind River Mountains, Wyoming. Zeitschrift für Gletscherkunde und Glacialogeologie 39, 161–181.

Mahaney, W.C., Dohm, J.M., Kapran, B., Hancock, R.G.V., Milner, M.W., 2009. Secondary Fe and Al in Antarctic paleosols: correlation to Mars with prospect for the presence of life. Icarus 203, 320–330.

Mahaney, W.C., Kalm, V., Hancock, R.G.V., Michel, F., Kapran, B., 2010a. Geochemistry and extractable Fe and Al in cold temperature soils of northwestern Siberia. Journal of Quaternary Science 25, 178–179.

Mahaney, W.C., Dohm, J.M., Costa, P., 2010b. Tsunamis on Mars: Earth analogues of projected Martian sediment. Planetary and Space Science 58, 1823–1831.

Marchant, D.R., Denton, G.H., Sugden, D.E., Swisher III, C.C., 1993. Miocene glacial stratigraphy and landscape evolution of the western Asgard Range, Antarctica. Geografisker Annaler 75A, 303–330.

McKeague, A., Day, J., 1966. Dithionite and oxalate extractable Fe and Al as aids in differentiating various classes of soils. Canadian Journal of Soil Science 46, 13–22.

Moore, D.M., Reynolds Jr., R.C., 1997. X-ray Diffraction and the Identification and Analysis of Clay Minerals. Oxford University Press, Oxford, UK. 378 pp.

Mustard, J.F., Murchie, S.L., Pelkey, S.M., Ehlmann, B.L., Milliken, R.E., Grant, J.A., Bibring, J.-P., Poulet, F., Bishop, J., Dobrea, E.N., Roach, L., Seelos, F., Arvidson, R.E., Wiseman, S., Green, R., Hash, C., Humm, D., Malaret, E., McGovern, J.A., Seelos, K., Clancy, T., Clark, R., Marais, D.D., Izenberg, N., Knudson, A., Langevin, Y., Martin, T., McGuire, P., Morris, R., Ronbinson, M., Roush, T., Smith, M., Swayze, G., Taylor, H., Titus, T., Wolff, M., 2008. Hydrated silicate minerals on Mars observed by the Mars Reconnaissance Orbiter CRISM instrument. Nature 454, 305–309.

National Soil Survey Center (NSSC), 1995. Soil Survey Laboratory Information Manual. Soil Survey Investigations Report no. 45, version 1.00, U.S.D.A. 305 pp.

Osterloo, M.M., Anderson, F.S., Hamilton, V.E., Hynek, B.M., 2010. Geologic context of proposed chloride-bearing materials on Mars. Journal of Geophysical Research 115, E10012. doi:10.1029/2010JE003613.

Oyama, M., Takehara, H., 1970. Standard Soil Color Charts. Japan Research Council for Agriculture, Forestry and Fisheries.

Parfitt, R.L., Childs, C.W., 1988. Estimation of forms of Fe and Al: a review and analysis of contrasting soils by dissolution and Moessbauer methods. Australian Journal of Soil Research 26, 121–144.

Parker, T.J., Gorsline, D.S., Saunders, R.S., Pieri, D.C., Schneeberger, D.M., 1993. Coastal geomorphology of the Martian northern plains. Journal of Geophysical Research 98, 11061–11078.

Pitt, J.I., 1979. The genus Penicillium and its teleomorphic states Eupenicillium and Talaromyces. Academic Press, London.

Scott, D.H., Dohm, J.M., Rice Jr., J.W., 1995. Map of Mars showing channels and possible paleolake basins. USGS Misc. Inv. Ser. Map I-2461 (1:30,000,000).

Thies, J.E., 2007. Molecular methods for studying soil ecology. In: Eldor, P.A. (Ed.), Soil Microbiology and Biochemistry. Elsevier Academic Press, Burlington MA. 96 pp.

Walker, A., 1981. The effects of magnetite on oxalate and dithionite-extractable iron. Soil Science Society of America Journal 47 (5), 1022–1026.

Wray, J.J., Murchie, S.L., Squyres, S.W., Seelos, F.P., Tornabene, L.L., 2009. Diverse aqueous environments on ancient Mars revealed in the southern highlands. Geology 37 (11), 1043–1046.

Wynn-Williams, D.D., Edwards, H.G.M., Newton, E.M., 2000. The detection of cold desert biomarkers, ancient and modern: Antarctica and Mars. Abstract Volume, The Second International Conference on Mars Polar Science and Exploration, Reykjavik, Iceland, pp. 182–183. August 21–25.

Zhou, J., Bruns, M.A., Tiedje, J.M., 1996. DNA recovery from soils of diverse composition. Applied and Environmental Microbiology 62 (2), 316–322.

Zuber, M.T., 2001. The crust and mantle of Mars. Nature 412, 220–227.